Nisula, Mikko; Linnera, Jarno; Karttunen, Antti J.; Karppinen, Maarit

Lithium Aryloxide Thin Films with Guest-Induced Structural Transformation by ALD/MLD

Published in:
CHEMISTRY: A EUROPEAN JOURNAL

DOI:
10.1002/chem.201605816

Published: 01/01/2017

Document Version
Peer reviewed version

Please cite the original version:
Nisula, M., Linnera, J., Karttunen, A. J., & Karppinen, M. (2017). Lithium Aryloxide Thin Films with Guest-Induced Structural Transformation by ALD/MLD. CHEMISTRY: A EUROPEAN JOURNAL, 2988 – 2992. https://doi.org/10.1002/chem.201605816

COMMUNICATION

Lithium aryloxide thin films with guest-induced structural transformation by ALD/MLD

Mikko Nisula, Jarno Linnera, Antti J. Karttunen, and Maarit Karppinen*[a]

Abstract: Crystalline Li-organic thin films are grown with the atomic/molecular layer deposition (ALD/MLD) technique from lithium hexamethyldisilazide and hydroquinone. The as-deposited films are found to undergo a reversible structural transformation upon exposure to ambient humid air. According to density functional theory calculations, the guest-induced transformation may be related to an unsaturated Li site in the crystal structure.

High-quality thin films of the (porous) coordination polymers (CPs) would be highly beneficial for applications in microelectronics, as e.g. sensors or smart membranes.[1] However, the present solution-based thin-film deposition methods of CPs may not be readily scalable for industrial production, whereas vapour-phase deposition would comply well with the needs of microelectronics fabrication processes.[2,3] Another potential difficulty arises from the fact that in the sensing applications it is beneficial for the thin-film material to contain open metal sites, i.e. metal nodes with an unsaturated coordination sphere to enhance the interaction towards guest molecules.[4] The inherent drawback of the solution-based synthesis methods is the unavoidable inclusion of the solvent molecules on these sites necessitating their often complicated post-deposition removal. Being intrinsically solvent-free, the vapour phase methods obviously circumvent this issue.

Atomic layer deposition (ALD) is a gas-phase thin film deposition technique with a well-established track record within the semiconductor industry. Owing to its unique deposition mechanism based on successive self-terminating surface reactions, the technique is well suited for the fabrication of conformal nanostructures on a wide range of substrate materials.[5] Moreover the emergence of the combined atomic/molecular layer deposition (ALD/MLD) technique now allows various metal constituents to be combined with organic moieties to yield hybrid inorganic-organic thin films.[6] Nevertheless, efforts to deposit porous CPs (also known as metal-organic frameworks or MOFs) utilizing gas-phase routes are scarce yet,[7,8] and only one direct ALD/MLD process to yield in-situ crystalline porous CP thin films has so far been reported.[9]

[a] M. Nisula, J. Linnera, Prof. A.J. Karttunen, Prof. M. Karppinen
Department of Chemistry and Materials Science
Aalto University
FI-00076, Aalto, Finland
E-mail: maarit.karppinen@aalto.fi

Supporting information for this article is given via a link at the end of the document.

Thus understanding the conditions leading to well-crystallized inorganic-organic thin films is a key requirement on the road to gas-phase deposition of porous CP thin films. In our very recent ALD/MLD works we have indeed been able to deposit in-situ crystalline (but not necessarily porous) inorganic-organic thin films with several different precursor combinations.[9–11] Especially with the s-block metals, Ca and Li, well-crystalline films were obtained over a wide temperature range when combined with 1,4-benzenedicarboxylic acid as the organic component. Of the s-block metals, lithium has probably been most extensively investigated as the active, undersaturated metal site in the field of coordination polymers,[12–15] and thus was chosen as the metal constituent in the present study as well. Since carboxylic acids tend to form rather stable compounds with lithium in tetrahedral coordination,[16,17] hydroquinone with its only two binding sites in para positions was chosen as the organic moiety on the basis that steric hindrance during the film deposition might prevent lithium from achieving the full coordination sphere.

In this study the lithium aryloxide thin films were deposited from lithium hexamethyldisilazide (LiHMDS, alternatively lithium bis(trimethylsilyl)amide) and hydroquinone (HQ) precursors using a commercial flow type F-120 ALD reactor from ASM Microchemistry (see ESI for full experimental details). The as-deposited films were uniform by visual observation; exposure to ambient air then led to a rapid colour change indicative of an increase in the film thickness while the uniformity in colour was well preserved. For the detailed study of the pristine samples, the films were coated with 40 ALD-cycles of Al_2O_3, which rendered the films stable for the duration of relevant experiments (confirmed by FTIR)

The film growth was studied in the temperature range of 105–280 °C (Figure 1a), at the low end limited by the sublimation temperature of HQ (95 °C), and at the high end by the drastic increase in the film roughness, which was taken as a sign of non-uniform growth. From 105 to 240 °C a rather monotonous decrease in the growth rate was observed, which is typical for the ALD/MLD processes of inorganic-organic hybrid materials.[6,18,19] The hallmark of ALD/MLD processes is the surface-saturation-limited growth, which manifests itself as a constant growth-per-cycle (GPC) value regardless of the precursor pulse lengths employed. Accordingly, this was verified for both the precursors at 120 and 220 °C (Figures 1b and 1c). Moreover, the film thickness was confirmed to increase in a highly linear manner as a function of the number of deposition cycles. In the FTIR spectrum of a pristine Al_2O_3-capped film from our Li-HMDS + HQ process, prominent absorption bands are seen only at 1500 cm^{-1} and below, attributable to the different modes of the benzene ring and the C-O bond. Importantly, the O-H stretching mode of the free HQ molecule expected at around 3700 cm^{-1} is absent for our thin films (Inset, Figure 2b).[20] It can thus be concluded that the HQ precursor has reacted completely to the expected aryloxide,

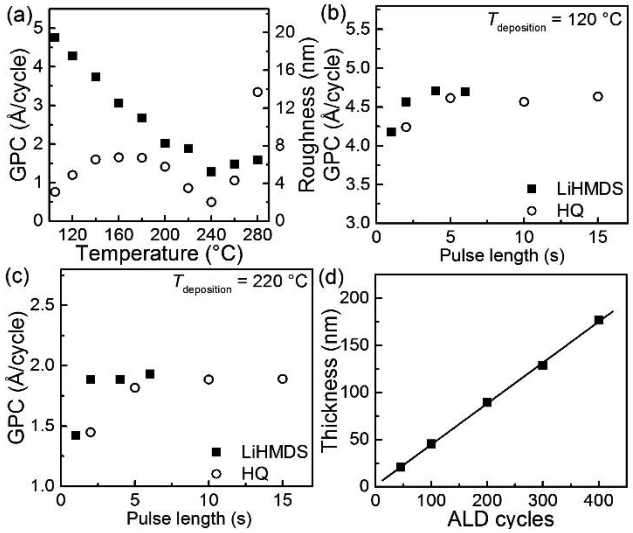

Figure 1. (a) The growth-per-cycle (GPC, solid squares) and roughness (open circles) of the Li_2Q thin films as a function of the deposition temperature, (b) and (c) the GPC as a function of the LiHMDS (solid squares) and HQ (open circles) pulse lengths determined at 120 and 220 °C, respectively, (d) the Li_2Q film thickness as a function of number of ALD/MLD cycles determined at deposition temperature of 120 °C.

i.e. dilithium 1,4-benzenediolate ($Li_2[p\text{-}C_6H_4O_2]$, hereafter Li_2Q). Also importantly, no signs of LiOH or Li_2CO_3 were detected either.

The as-deposited Li_2Q thin films were crystalline at all deposition temperatures as verified by grazing incidence X-ray diffraction (GIXRD) (Figure S1, ESI). With increasing deposition temperature, a change in the GIXRD patterns can be observed: the peak at 11.5° diminishes, while a new peak appears at 23.3°. The density of the films, as determined by XRR, however stays rather constant at 1.2 g/cm^3. More detailed diffraction patterns were measured from ca. 800 nm thick samples deposited at 105 and 220 °C. At the low-temperature end, a well-defined pattern could be obtained (Figure 2a), whereas the high-temperature sample yielded only a few reflections which partially overlapped with those of the low-temperature sample (Figure S2, ESI). Importantly, once formed, the low-temperature sample retains its crystal structure even at elevated temperatures as was investigated through a post-deposition heat treatment at 250 °C in vacuum.

To the best of our knowledge, no prior reports exist on the crystal structure of Li_2Q or related Li-based compounds. However, in bulk samples HQ is known to form crystalline structures with Ti[21] and alkali metals[22] other than Li. Most importantly, $Na_2[p\text{-}C_6H_4O_2]$ and $K_2[p\text{-}C_6H_4O_2]$ (hereafter Na_2Q and K_2Q, respectively) are reported to be isostructural. Thus by assuming that Li_2Q would share the same structural motif, the atomic-level structure of the corresponding Li_2Q compound was predicted using density functional theory (PBE0/TZVP, computational details are described in full detail in the ESI).[23–29]

Initial optimization of Li_2Q using the space group $P4_2/ncm$ and atomic positions from the Na_2Q data of Couhorn and Dronskowski[22] ended up in a transition state characterized by a single imaginary frequency (64*i* cm^{-1}). Changing the geometry in the direction of the normal modes of the imaginary frequency reduced the symmetry to the orthorhombic subgroup *Pccn,* and the subsequent optimization resulted in a true local minimum accompanied with a total energy reduction of 9 kJ/mol per unit cell. The calculated structural parameters are listed in Table S2 in ESI. The structure, shown in the inset of Figure 2a, is still closely similar to that of Na_2Q and K_2Q, and the predicted lattice parameters are: *a* = 11.49 Å, *b* = 10.38 Å, *c* = 4.74 Å. In this structure, infinite Li_2O_2 pillars running along the c-axis are interconnected by the bidentate $C_6H_4O_2^{2-}$ units with each Li atom coordinated to three oxygen atoms (Figure S3, ESI). The length of the c-axis for our Li_2Q falls perfectly in line with those reported for the Na and K analogues when these values are plotted against the ionic radius of the alkali metal (Figure S4, ESI). On the contrary, the *a* and *b* lattice parameters are comparatively larger; this is because in Na_2Q and K_2Q the benzene ring lies more parallel in respect to the M_2O_2 chain. In the case of Li_2Q the shorter Li-O bonds lead to a less distorted chain and consequently, the C-O bond in the oxygen tetrahedron points to a more outwards

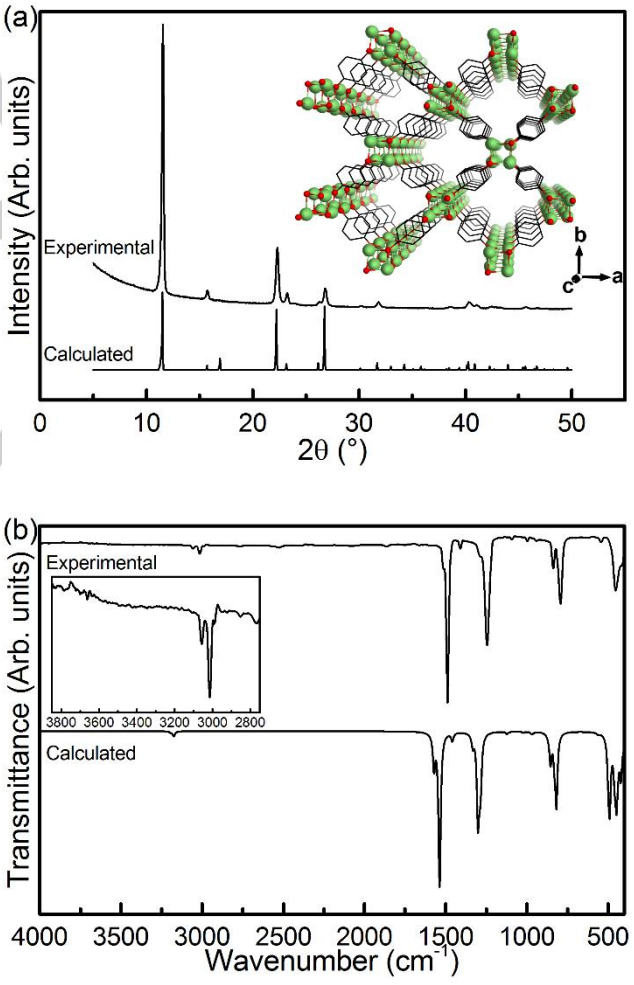

Figure 2. Comparisons between (a) the experimental and calculated X-ray diffraction patterns (the inset shows the proposed crystal structure of the Li_2Q thin films along the c-axis; the structure was drawn using the VESTA software), and (b) the experimental and calculated IR spectra, for our Li_2Q thin films.

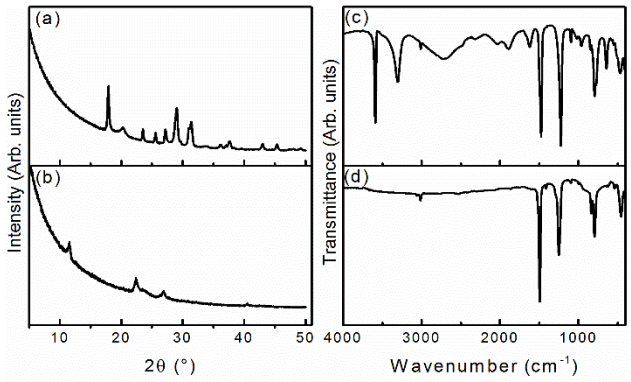

Figure 3. GIXRD patterns of Li_2Q samples (a) after exposure to ambient air, and (b) after drying; (c) and (d) are the corresponding IR spectra.

direction. The orientation of the benzene ring in relation to the Li_2O_2 chain also explains the shift to the orthorhombic symmetry. The undercoordinated Li with a positive charge interacts with the delocalized negative charge of the $C_6H_4O_2^{2-}$ anion. As the $C_6H_4O_2^{2-}$ anion has a rotational degree of freedom about its centre axis, it is energetically more favourable for it to twist so that the opposing corners of the benzene rings are closest to the adjacent Li ions. Consequently, the corresponding carbon atoms exhibit a somewhat higher negative charge than the other members of the ring.

The Li-O bond lengths (1.90–1.94 Å) are very close to those reported for structurally similar lithium phenolate cubane clusters (1.91–1.98 Å).[30] Also the C-O lengths are essentially equal in the two structures (1.34 Å and 1.33 Å for Li_2Q and Li-phenolate, respectively),[30] which implies of charge localization on the oxygen atom of equal magnitude.[31] When compared to the experimental data, the calculated diffraction pattern matches very closely to the experimental one (Figure 2a) and Le Bail fitting (Figure S5, ESI) in space group *Pccn* yields an excellent fit with lattice parameters very close to the predicted values: a = 11.25 Å, b = 10.45 Å, c = 4.66 Å. The original tetragonal structure isotypic to Na_2Q was also evaluated, but this resulted in a markedly poorer fit (Figure S6, ESI).

Figure 2b shows further validation of the structure as the theoretical IR spectrum produces all the IR absorption bands that appear in the experimental spectrum (full interpretation of the vibrational modes in Table S2, ESI). The small systematic differences in peak positions between the theoretical and experimental spectra can be attributed to the harmonic approximation used in the calculations. Main features in the lower wavenumbers (1100–400 cm^{-1}) arise from the different stretching and bending modes of Li and the benzene ring and the higher wavenumber (1600–1200 cm^{-1}) peaks stem from the stretching of C=C and C-O bonds. Characteristic aromatic C-H stretching vibrations are also visible as small peaks just above 3000 cm^{-1}.

The poor quality of the diffraction data for the high-temperature sample prevented a more detailed study of its crystal structure. The pattern cannot however be explained by the structure proposed for the low-temperature Li_2Q phase.

When the samples were exposed to ambient atmosphere without the protective Al_2O_3 coating, a drastic change in the GIXRD pattern could be observed (Figure 3a). Afterwards, the newly formed phase was rather stable in ambient air with a slow deterioration in crystallinity on a time scale of several months. This was accompanied by a possible formation of Li_2CO_3 as determined from the IR data. Similarly, in the IR spectrum of the air-exposed sample (Figure 3c), several new absorption bands are observed. Again the spectrum does not match those of LiOH and Li_2CO_3. The strong bands at 3590 and 3304 cm^{-1} indicate the presence of free and hydrogen bonded -OH groups, respectively.[32] Additionally, the band at 1621 cm^{-1} might arise from the H-O-H bending mode. However, the bands between 2000 and 3000 cm^{-1} could not be identified. Hydrogen bonding, especially in confined environments with short interaction distances may cause red shifting and broadening of absorption bands in the magnitude of hundreds of reciprocal centimetres, which complicates the identification.[32] Atomic force microscopy (AFM) images taken from pristine (Figure S7a, ESI) and exposed (Figure S7b, ESI) samples showed an evolution in the RMS roughness from 2.9 to 7.8 nm. The apparent increase in the crystallite size might imply the expansion of the unit cell size upon exposure.

Interestingly, the transformation appears to be reversible. When the exposed samples were heated in vacuum at 120 °C, and then capped with Al_2O_3, the FTIR spectrum was found to revert back to the pristine one (Figure 3d) and at the same time the GIXRD pattern (Figure 3b) indicated that the original phase had been recovered although the crystallinity did somewhat suffer. Optical band gap as determined by UV-vis spectroscopy (Figure S8, ESI), was found to be essentially similar for the pristine (3.67 eV) and the air-exposed sample (3.64 eV).

The proposed structure would reasonably explain the observed behaviour upon the exposure to ambient air. The undercoordinated lithium atoms in pristine Li_2Q would readily complete their coordination spheres by absorption of water molecules. Unfortunately we could not adequately solve the crystal structure of the exposed sample by merely placing water molecules at the open metal sites. Although multiple different geometries were considered with varying amount of water molecules, the theoretical diffraction pattern never quite matched the experimental at a satisfactory degree. This is likely because of all the empty space in the material and the vast number of possible configurations H_2O can occupy the structure. A single static geometry is unlikely to produce the diffraction pattern of a structure that can contain free water molecules and is thus prone to rapid ligand exchange

Given the observed reactivity of the samples, it seems that the gas-phase deposition method did indeed avert the issue of solvent-molecule inclusion in the unsaturated metal sites. In the case of vapour-phase synthesis investigated in the present work, such 'solvent' molecule would either be one of the precursors or the side product of the reaction, bis(trimethylsilyl)amine ($[(CH_3)_3Si]_2NH$). As none of these alternatives appear in the FTIR spectrum of the pristine sample, it seems that either they are unable to act as guest molecules or the synthesis conditions prevent their absorption. Although we were unable to determine the porosity of our coordination network material, the present findings might be relevant also in the field of metal-organic frameworks. An interesting concept, though not tried here, would be to functionalize the as-deposited films with some suitable guest

molecule prior to the exposure to ambient air. Moreover, as the Li_2Q phase was reported to be unattainable through solution based methods,[22] our results can be taken as a promising demonstration of the advantage of vapor phase methods on the synthesis of novel coordination polymers.

Regarding the crystallization of ALD/MLD samples, it is interesting to notice that including the present findings, all the reported ALD/MLD processes for s-block metals have yielded crystalline thin films over wide temperature windows,[10,11,33] whereas the transition metal and aluminium based processes, with the exception of Cu-terephthalate[9] have resulted in amorphous thin films. The s-block metals are known to form mainly ionic compounds with organic constituents.[34] The non-directionality of the ionic bond might be advantageous for the crystallization of the films during the film growth as it might give the molecules more freedom for proper orientation. Or the other way around, the more directional covalent bonds of transition metals may force the organic constituent to an unsuitable angle for the formation of a well-defined structure. Also the deposition temperature appears to play a significant role with low temperature being seemingly more favourable for thin films with high crystallinity.

In conclusion, we have successfully deposited crystalline thin films of lithium aryloxide through an ALD/MLD process for which all the hallmarks of the expected atomic/molecular layer-by-layer growth could be demonstrated. According to DFT calculations the crystal structure of the new Li-based hybrid material appears to be closely related to those previously reported for bulk samples of Na_2Q and K_2Q. Most interestingly, the as-grown Li_2Q thin films were found to undergo a reversible structural transformation associated with their reaction with ambient humid air. The reactivity of the films could be ascribed to the coordinatively-undersaturated Li site in the Li_2Q structure promoting strong interaction with the guest molecules. While the reversibility of the absorption reaction is not ideal for the present compound, we believe that our findings should serve as a strong foothold for the development of gas-phase layer-by-layer synthesis of coordination network materials with advanced functionalities.

Acknowledgements

The present work has received funding from the European Research Council under the European Union's Seventh Framework Programme (FP/2007-2013)/ERC Advanced Grant Agreement (No. 339478), and also from the Academy of Finland (Nos. 296299 and 303452). Mr. Panagiotis Spiliopoulos and Prof. Eero Kontturi are thanked for the AFM images.

Keywords: Coordination polymer • Lithium organic hybrid • Thin film • Atomic layer deposition • Molecular layer deposition

[1] D. Zacher, O. Shekhah, C. Wöll, R. A. Fischer, *Chem. Soc. Rev.* **2009**, *38*, 1418–1429.
[2] I. Stassen, D. De Vos, R. Ameloot, *Chem. - A Eur. J.* **2016**, *22*, 14452–14460.
[3] M. D. Allendorf, A. Schwartzberg, V. Stavila, A. A. Talin, *Chem. - A Eur. J.* **2011**, *17*, 11372–11388.
[4] L. E. Kreno, K. Leong, O. K. Farha, M. Allendorf, R. P. Van Duyne, J. T. Hupp, *Chem. Rev.* **2011**, *112*, 1105–1125.
[5] S. M. George, *Chem. Rev.* **2010**, *110*, 111–131.
[6] P. Sundberg, M. Karppinen, *Beilstein J. Nanotechnol.* **2014**, *5*, 1104–1136.
[7] I. Stassen, M. Styles, G. Grenci, H. Van Gorp, W. Vanderlinden, S. De Feyter, P. Falcaro, D. De Vos, P. Vereecken, R. Ameloot, *Nat. Mater.* **2015**, *15*, 304–310.
[8] K. B. Lausund, O. Nilsen, *Nat. Commun.* **2016**, *7*, 13578.
[9] E. Ahvenniemi, M. Karppinen, *Chem. Commun.* **2015**, *52*, 1139–1142.
[10] E. Ahvenniemi, M. Karppinen, *Chem. Mater.* **2016**, *28*, 6260–6265.
[11] M. Nisula, M. Karppinen, *ACS Nano Lett.* **2016**, *16*, 1276–1281.
[12] K. L. Mulfort, O. K. Farha, C. L. Stern, A. A. Sarjeant, J. T. Hupp, *J. Am. Chem. Soc.* **2009**, *131*, 3866–3868.
[13] L. H. Xie, J. Bin Lin, X. M. Liu, Y. Wang, W. X. Zhang, J. P. Zhang, X. M. Chen, *Inorg. Chem.* **2010**, *49*, 1158–1165.
[14] R. El Osta, M. Frigoli, J. Marrot, N. Guillou, H. Chevreau, R. I. Walton, F. Millange, *Chem. Commun.* **2012**, *48*, 10639–10641.
[15] D. Banerjee, S. J. Kim, W. Li, H. Wu, J. Li, L. a. Borkowski, B. L. Philips, J. B. Parise, *Cryst. Growth Des.* **2010**, *10*, 2801–2805.
[16] D. Banerjee, J. B. Parise, *Cryst. Growth Des.* **2011**, *11*, 4704–4720.
[17] U. Olsher, R. M. Izatt, J. S. Bradshaw, N. K. Dalley, *Chem. Rev.* **1991**, *91*, 137–164.
[18] P. Sundberg, M. Karppinen, *Eur. J. Inorg. Chem.* **2014**, 968–974.
[19] B. H. Lee, B. Yoon, A. I. Abdulagatov, R. a. Hall, S. M. George, *Adv. Funct. Mater.* **2013**, *23*, 532–546.
[20] A. J. Karttunen, T. Tynell, M. Karppinen, *J. Phys. Chem. C* **2015**, *119*, 13105–13114.
[21] T. P. Vaid, E. B. Lobkovsky, P. T. Wolczanski, C. U. V, **1997**, *7863*, 8742–8743.
[22] U. Couhorn, R. Dronskowski, *Z. Anorg. Allg. Chem.* **2003**, *629*, 647–652.
[23] R. Dovesi, R. Orlando, A. Erba, C. M. Zicovich-Wilson, B. Civalleri, S. Casassa, L. Maschio, M. Ferrabone, M. De La Pierre, P. D'Arco, Y. Noël, M. Causà, M. Rérat, B. Kirtman, *Int. J. Quantum Chem.* **2014**, *114*, 1287–1317.
[24] R. Dovesi, V. R. Saunders, C. Roetti, R. Orlando, C. M. Zicovich-Wilson, F. Pascale, B. Civalleri, K. Doll, N. M. Harrison, I. J. Bush, P. D'Arco, M. Llunell, M. Causà, Y. Noël, CRYSTAL14 User's Manual, University of Torino, Torino, Italy, **2004**.
[25] F. Pascale, C. M. Zicovich-Wilson, F. López Gejo, B. Civalleri, R. Orlando, R. Dovesi, *J. Comput. Chem.* **2004**, *25*, 888–897.
[26] C. M. Zicovich-Wilson, F. Pascale, C. Roetti, V. R. Saunders, R. Orlando, R. Dovesi, *J. Comput. Chem.* **2004**, *25*, 1873–1881.
[27] J. P. Perdew, K. Burke, M. Ernzerhof, *Phys. Rev. Lett.* **1996**, *77*, 3865–3868.
[28] C. Adamo, V. Barone, *J. Chem. Phys.* **1999**, *110*, 6158–6170.
[29] F. Weigend, R. Ahlrichs, *Phys. Chem. Chem. Phys.* **2005**, *7*, 3297–3305.
[30] T. S. De Vries, A. Goswami, L. R. Liou, J. M. Gruver, E. Jayne, D. B. Collum, *J. Am. Chem. Soc.* **2009**, *131*, 13142–13154.
[31] S. Tominaka, H. H.-M. Yeung, S. Henke, A. K. Cheetham, *CrystEngComm* **2016**, *18*, 398–406.
[32] T. Steiner, *Angew. Chemie Int. Ed.* **2002**, *41*, 48–76.
[33] Z. Giedraityte, O. Lopez-Acevedo, L. A. Espinosa Leal, V. Pale, J. Sainio, T. S. Tripathi, M. Karppinen, *J. Phys. Chem. C* **2016**, *120*, 26342–26349 (2016).
[34] K. M. Fromm, *Coord. Chem. Rev.* **2008**, *252*, 856–885.

Entry for the Table of Contents (Please choose one layout)

Layout 1:

COMMUNICATION

From precursor vapours to crystalline hybrid thin films: Atomic/molecular layer deposition allows the layer-by-layer vapour-phase growth of highly crystalline coordination polymer thin films. Benefiting from the unsaturated metal sites the novel lithium aryloxide structure is capable to reversibly react with guest molecules.

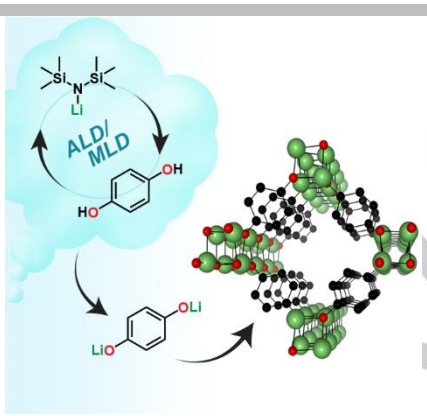

*Mikko Nisula, Jarno Linnera, Antti J. Karttunen, and Maarit Karppinen**

Page No. – Page No.

Lithium aryloxide thin films with guest-induced structural transformation by ALD/MLD